VI-Sintered alumina/corundum (Al_2O_3)

Appearance and Causes

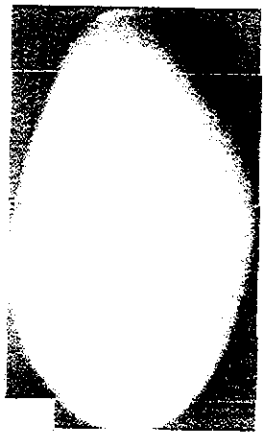

Figure 23: Sintered corundum (denser fine grained)

a-Dense/opaque inclusions.
b-Tightly packed crystalline structure.
c-Absence of bubbles.
d-Little/no reaction fringe or ream sac around the stone.
e-White/colorless in incident light.
causes of this defect are:
1-Disintegration/spalling of high alumina refractories e.g. thermocouple sheaths, oxygen probes.
2-Wear/breakdown of (castable) burner blocks.
3-Batch and cullet contamination – sintered alumina is often used as wear resistant material. Also in abrasive materials and grinding wheels.

VII-Nepheline ($Na_2OAl_2O_3SiO_2$)

Appearance and Causes

Figure 24: Nepheline

a-Semi transparent/glassy stones
b-Generally rounded or elongated
c-White/pale brown in reflected light.
d-Heavy ream sac is common.
e-Absence of bubbles – within or around the stone.
f-Fine grain crystals or transparent plates.
Causes of such inclusions are:
1-Alkali attack on any alumina-silica containing refractory.
2-Nepheline will form on firebricks, on high alumina and fusion cast AZS refractories.
3-Often associated with refractory contamination of *cullet/raw materials.*

VIII-Ream knots

Appearance and Cause

Bubble from the last stage of dissolution of firebrick refractory.

Zirconia recrystalizing from surface rundown of AZS superstructure brick.

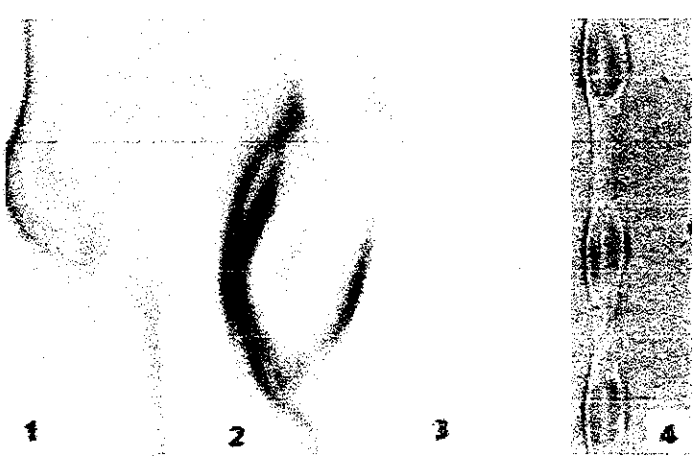

Nos. 1 and 2 are typical of a melter/batch contamination origin, 3 "line" and 4 "stitchline" are usually traceable to running furnace refractories.

Figure 25: Different types of ream knots

a-Transparent, usually colorless "drops" or lines of clear glass visible against the surrounding glass. Many have their own characteristic shape as shown in the figure
b-Surface distortion of the glass.
c-Gas bubble – particularly in the "knot" or body of the sac.
d-Traces of original or recrystallized material.

Cause of this defect is:
Dissolution of minerals into the glass. These minerals comes from refractories, contaminations of the raw materials, and/ or rundown from superstructure refractories in the furnace.

C-Contamination origin

I-Sand chromite

Appearance and Cause

Figure 26: Typical sand chromite showing rounding of the edges.

a-Distinct characteristic black to dark green single grains – typically rounded and small similar to sand grain size (0.5mm).
b-Random distribution.

The cause of this defect is the presence of chromite indigenously in many glassmaking sands.

II-Iron metal

Appearance and Causes

Figure 27: Iron metal (note the brown color band in the glass)

a-Rounded opaque, grey/black shiny reflective metallic pellets.
b-Green/brown colored streaks in the surrounding glass.
c-Gas bubbles.

Causes of this defect are:

1-*Contamination of batch or cullet by steel.*
2-Corrosion of furnace steelwork.

3.1.3 Tin related defects

I- Cassiterite (tin oxide SnO_2)

Appearance and Causes

Figure 28: Cassiterite

a-Dense opaque agglomerates of granular structure.
b-The color is dense-white/opalescent in incident light.
c-Colorless to black in transmitted light.
d-Absence of ream sac.
e-Absence of bubble.

Causes of this defect are:

1-Most cassiterite stones arise from condensation of tin oxide vapors around the float tweel/canal superstructure and bath lintel areas.
2-Cullet contamination (especially after float bath upset).
3-Recrystallization, within the furnace, produces typical granular structures

II-Float bath faults

Appearance and Causes

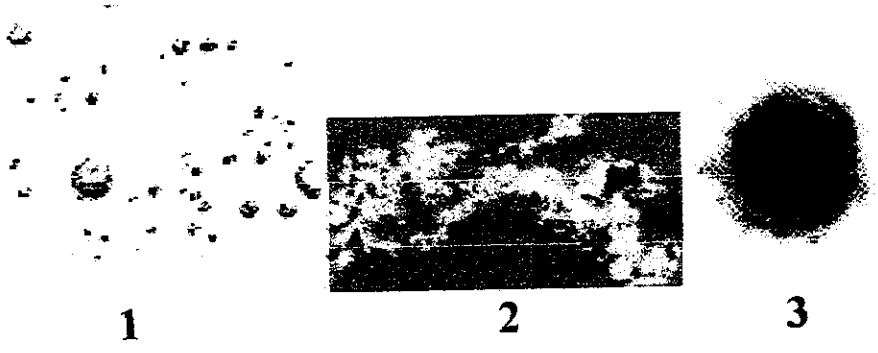

Figure 29: 1-Top tin (top surface), 2-Tin-Pickup (bottom surface) and 3-Top tin speck (top surface)

Defects derived from the float bath are normally surface related. They occur on both top and bottom surfaces but, apart from bubble from the wetback, never in the body of the ribbon. They can originate from different parts of the float bath.

Causes of these defects are:

1-Float bath upsets
2-Temperature changes in float bath out of normal settings
3-Mechanical movements of float bath equipments
4-Bad bath sealing

3.2 Chemical analysis using x-rays

3.2.1 Relation between glass composition and ream

Using x-ray fluorescence, the composition of glass was analyzed during the period of study. It was noted that some ream changes are accompanied with some changes in the composition of glass, and this can be noted obviously by the main oxides of glass.

The ream values as described before are taken every 100 mm across the ribbon saleable width, where the standard saleable width is 3210 mm (see table 2), graded from 0 (no ream) to 7 (severe).

The variations of oxide percentage (in glass composition) in left, center and right positions of the glass ribbon are related to the ream values variations in these positions as shown in tables 3, 4, 5, 6, 7, 8, 9 & 10

Table 2 :REAM VALUES ACROSS THE SALEABLE WIDTH IN THE SELECTED SAMPLES BEGAINING FROM LEFT EDGE OF THE RIBBON

position in ribbonx100mm	1	2	3	4	5	6	7	8	9	10	11	12	13	14	15	16	17	18	19	20	21	22	23	24	25	26	27	28	29	30	31	32
30/04/2002	5	4	1	1	1	0	0	0	0	0	0	0	0	0	0	2	0	0	0	0	0	0	0	0	0	0	0	0	0	0	0	3
30/05/2002	2	1	0	2	0	0	0	0	0	0	0	0	0	0	1	2	1	0	0	0	0	0	0	0	0	0	1	1	1	1	1	2
30/06/2002	3	2	0	0	0	0	0	0	0	0	0	0	0	0	1	0	0	0	0	0	0	0	0	0	0	0	0	0	1	1	5	2
28/07/2002	3	1	1	1	1	1	0	0	0	0	0	0	0	0	0	1	0	0	0	0	0	0	0	0	0	0	1	2	2	1	2	2
30/08/2002	3	2	4	1	0	0	0	0	0	0	0	0	0	0	0	0	2	1	0	0	0	0	0	0	1	0	0	0	0	1	4	2
16/09/2002	4	4	3	2	3	2	3	0	0	0	0	0	0	0	0	0	0	0	0	0	0	0	0	0	0	0	0	3	0	3	6	6
07/10/2002	6	4	6	5	6	7	7	7	7	7	7	7	6	4	5	5	4	5	5	6	3	5	4	5	4	5	1	1	1	0	0	2
08/10/2002	0	0	0	0	0	0	0	0	2	2	4	4	4	4	3	5	3	5	3	3	2	1	1	1	1	1	1	1	1	1	2	1

Note : The shadowed values represent the positions from which samples for x-ray composition analysis were cut

Table 3: Variations of the main oxides percentages (in glass composition) and ream values in left, center & right positions in glass ribbon in the sample of 30/4/2002

			30/04/2002		
			REAM VALUE		
			CENTER	RIGHT	LEFT
			0	0	4
OXIDE %	FLUXING OXIDE	Na_2O	13.79	13.79	13.73
	STABILIZING OXIDES	CaO	8.570	8.569	8.506
		MgO	3.935	3.934	3.924
	FORMER OXIDE	SiO_2	72.41	72.41	72.55
	SUM. OF STABILIZING OXIDES PERCENTAGES		12.505	12.503	12.430

Table 4: Variations of the main oxides percentages (in glass composition) and ream values in left, center & right positions in glass ribbon in the sample of 30/5/2002

			30/05/2002		
			REAM VALUE		
			LEFT	RIGHT	CENTER
			1	1	2
OXIDE %	FLUXING OXIDE	Na_2O	13.77	13.77	13.64
	STABILIZING OXIDES	CaO	8.646	8.642	8.668
		MgO	3.915	3.91	3.894
	FORMER OXIDE	SiO_2	72.37	72.40	72.52
	SUM. OF STABILIZING OXIDES PERCENTAGES		12.561	12.552	12.562

Table 5: Variations of the main oxides percentages (in glass composition) and ream values in left, center & right positions in glass ribbon in the sample of 30/6/2002

			30/06/2002		
			REAM VALUE		
			CENTER	LEFT	RIGHT
			0	2	5
OXIDE %	FLUXING OXIDE	Na_2O	13.73	13.66	13.62
	STABILIZING OXIDES	CaO	8.604	8.592	8.555
		MgO	3.896	3.877	3.868
	FORMER OXIDE	SiO_2	72.47	72.57	72.65
	SUM. OF STABILIZING OXIDES PERCENTAGES		12.5	12.469	12.423

Table 6: Variations of the main oxides percentages (in glass composition) and ream values in left, center & right positions in glass ribbon in the sample of 28/7/2002

			28/07/2002		
			REAM VALUE		
			CENTER	LEFT	RIGHT
		OXIDE %	1	1	2
OXIDE %	FLUXING OXIDE	Na_2O	13.80	13.79	13.78
	STABILIZING OXIDES	CaO	8.726	8.702	8.711
		MgO	3.963	3.970	3.945
	FORMER OXIDE	SiO_2	72.25	72.26	72.30
	SUM. OF STABILIZING OXIDES PERCENTAGES		12.689	12.672	12.656

Table 7: Variations of the main oxides percentages (in glass composition) and ream values in left, center & right positions in glass ribbon in the sample of 30/8/2002

			30/08/2002		
			REAM VALUE		
			LEFT	CENTER	RIGHT
			2	2	4
OXIDE %	FLUXING OXIDE	Na_2O	13.77	13.78	13.70
	STABILIZING OXIDES	CaO	8.641	8.627	8.576
		MgO	3.964	3.965	3.915
	FORMER OXIDE	SiO_2	72.21	72.21	72.41
	SUM. OF STABILIZING OXIDES PERCENTAGES		12.605	12.592	12.491

Table 8: Variations of the main oxides percentages (in glass composition) and ream values in left, center & right positions in glass ribbon in the sample of 16/9/2002

			16/09/2002		
			REAM VALUE		
			CENTER	LEFT	RIGHT
			0	3	6
OXIDE %	FLUXING OXIDE	Na_2O	13.91	13.89	13.82
	STABILIZING OXIDES	CaO	8.672	8.602	8.636
		MgO	3.965	3.958	3.914
	FORMER OXIDE	SiO_2	72.01	72.11	72.24
	SUM. OF STABILIZING OXIDES PERCENTAGES		12.637	12.56	12.55

Table 9: Variations of the main oxides percentages (in glass composition) and ream values in left, center & right positions in glass ribbon in the sample of 7/10/2002

			07/10/2002		
			REAM VALUE		
			RIGHT	LEFT	CENTER
			1	6	7
OXIDE %	FLUXING OXIDE	Na_2O	13.19	12.85	12.82
	STABILIZING OXIDES	CaO	7.793	7.573	7.550
		MgO	3.558	3.507	3.408
	FORMER OXIDE	SiO_2	74.33	74.91	75.07
	SUM. OF STABILIZING OXIDES PERCENTAGES		11.351	11.08	10.958

Table 10: Variations of the main oxides percentages (in glass composition) and ream values in left, center & right positions in glass ribbon in the sample of 8/10/2002

			08/10/2002		
			REAM VALUE		
			LEFT	RIGHT	CENTER
		OXIDE %	0	2	5
OXIDE %	FLUXING OXIDE	Na_2O	13.69	13.61	13.56
	STABILIZING OXIDES	CaO	8.625	8.606	8.584
		MgO	3.992	3.980	3.982
	FORMER OXIDE	SiO_2	72.39	72.50	72.57
	SUM. OF STABILIZING OXIDES PERCENTAGES		12.617	12.586	12.566

From the above results in the tables it can be noted that for the same sample as the ream value increases in a position of the glass ribbon the former oxide SiO_2 % increases, the fluxing oxide Na_2O % decreases, in most of samples CaO% & MgO % decreases slightly & the summation of stabilizing oxides percentages (CaO& MgO) also decreases.

3.2.2 X-ray analysis of glass samples containing stones

X-ray fluorescence spectrometer was used to analyze the *full constituents of the glass samples containing* stones.

The following table 5 gives the normal composition of homogeneous, ream free glass during the period of months from April to October 2002 and the average of that composition during the mentioned period:

Table 11: the composition of normal stone-free glass during the period of months from April to October 2002 and the average of that composition during the mentioned period (Note: Results were given by x-ray fluorescence analysis of glass)

Month	Na_2O (%)	MgO (%)	Al_2O_3 (%)	SiO_2 (%)	SO_3 (%)	K_2O (%)	CaO (%)	TiO_2 (%)	Fe_2O_3 (%)
APRIL	13.69	3.975	0.695	72.44	0.283	0.014	8.609	0.027	0.102
MAY	13.84	3.958	0.707	72.33	0.273	0.012	8.573	0.030	0.112
JUNE	13.75	3.937	0.708	72.34	0.240	0.058	8.675	0.030	0.102
JULY	13.70	3.901	0.773	72.46	0.260	0.014	8.575	0.032	0.120
AUG.	13.93	3.920	0.767	72.20	0.274	0.043	8.556	0.032	0.111
SEPT.	13.83	3.935	0.776	72.19	0.283	0.060	8.626	0.027	0.097
OCT.	13.49	3.970	0.736	72.58	0.278	0.019	8.631	0.029	0.106
AVG.	13.75	3.942	0.737	72.36	0.270	0.031	8.606	0.030	0.107

As mentioned before, the analysis is that for the glass containing stone, where the difference between normal glass composition and glass containing stone composition can be distinguished.

The percentages given of the oxides (although they are not the exact composition of the stone) can yield useful qualitative information about this stone.

The following are the results of x-ray analysis of the stone samples compared with the average normal glass composition.

1-Silica scum

Table 12: X-ray analysis of a sample containing silica scum

OXIDE	Na_2O	MgO	Al_2O_3	SiO_2	SO_3	K_2O	CaO	TiO_2	Fe_2O_3
SAMPLE COMPOSITION (%)	10.10	1.507	0.413	84.90	0.123	0.166	2.680	0.020	0.081
AVG. NORMAL GLASS COMPOSITION (%)	13.75	3.942	0.737	72.36	0.270	0.031	8.606	0.030	0.107

The analysis shown in the table indicates that the percentages of both SiO_2 and K_2O in glass are higher than the normal composition. On the other hand the percentages of the remaining oxides are much lower than the normal composition. This inclusion was taken as a sample after a batch plant problem of incorrect weighing of raw materials causing melting upset.

2-Silica layer (cristabolite)

Table 13: X-ray analysis of a sample containing cristabolite

OXIDE	Na_2O	MgO	Al_2O_3	SiO_2	SO_3	K_2O	CaO	TiO_2	Fe_2O_3
SAMPLE COMPOSITION (%)	13.27	3.786	0.700	73.42	0.212	0.060	8.323	0.030	0.092
AVG. NORMAL GLASS COMPOSITION (%)	13.75	3.942	0.737	72.36	0.270	0.031	8.606	0.030	0.107

The analysis of this inclusion shows a slight increase in SiO_2% more than the normal accompanied with decrease in Na_2O%, MgO% and CaO%. This inclusion was taken as a sample after silica scum problem (melting upset), where silica layer problems follow major melting upsets and continue over several weeks – as the defect is released from the furnace working end, (where cristabolite is devitrifying in the working end-not the melt end-of the furnace).

3-Silica layer (tridymite)

Table 14: X-ray analysis of a sample containing tridymite

OXIDE	Na_2O	MgO	Al_2O_3	SiO_2	SO_3	K_2O	CaO	TiO_2	Fe_2O_3
SAMPLE COMPOSITION (%)	13.24	3.939	0.658	72.60	0.241	0.018	9.060	0.037	0.096
AVG. NORMAL GLASS COMPOSITION (%)	13.75	3.942	0.737	72.36	0.270	0.031	8.606	0.030	0.107

The analysis of the inclusion shows an increase in both CaO% & SiO_2 % accompanied with a decrease in Na_2O%. Tridmyte comes from devitrification in the canal and the defect appeared in a period of load changes.

4-Ream knots in glass

Table 15: X-ray analysis of a sample containing ream knots

OXIDE	Na_2O	MgO	Al_2O_3	SiO_2	SO_3	K_2O	CaO	TiO_2	Fe_2O_3
SAMPLE COMPOSITION (%)	13.81	3.989	0.823	72.03	0.233	0.135	8.736	0.029	0.104
AVG. NORMAL GLASS COMPOSITION (%)	13.75	3.942	0.737	72.36	0.270	0.031	8.606	0.030	0.107

The analysis of the inclusion shows an increase in Al_2O_3% indicating that the source of the ream knot is alumina-containing source (aluminous fire brick). The analysis also shows an increase in K_2O% and a decrease in SiO_2%.

Note: In the case of the pervious last three samples, the variations from the normal composition are not too high because the samples analyzed were small in their size compared with their surrounding glass.

5-Super structure rundown

Table 16: X-ray analysis of a sample containing super structure rundown

OXIDE	Na_2O	MgO	Al_2O_3	SiO_2	SO_3	K_2O	CaO	TiO_2	Fe_2O_3
SAMPLE COMPOSITION (%)	11.91	3.893	11.440	65.39	0.239	0.060	6.803	0.029	0.124
AVG. NORMAL GLASS COMPOSITION (%)	13.75	3.942	0.737	72.36	0.270	0.031	8.606	0.030	0.107

The analysis of the inclusion shows high increase in Al_2O_3% accompanied with significant decrease in SiO_2%, Na_2O% and CaO. The nearest typical chemical composition to this defect is that for a type of low-silica brick, which is used in non-glass contact areas (note alumina & silica percentages in the following table):

Table 17: Typical chemical composition for a type of low-silica brick

OXIDE	SiO_2	Al_2O_3	CaO	MgO	Fe_2O_3
%	74.5	20.5	0.2	0.1	0.4

(Reference: Fay.V.Tooley, "The Hand Book of Glass Manufacture", 3rd edition, Ashlee New York (1984).

Difference between the typical composition of the refractory and the given composition by the sample analysis is due to the surrounding glass around the defect.

6-High alumina (mullite)

Table 18: X-ray analysis of a sample containing high alumina refractory

OXIDE	Na_2O	MgO	Al_2O_3	SiO_2	SO_3	K_2O	CaO	TiO_2	Fe_2O_3
SAMPLE COMPOSITION (%)	11.53	3.103	38.380	41.13	0.930	0.068	4.606	0.022	0.116
AVG. NORMAL GLASS COMPOSITION (%)	13.75	3.942	0.737	72.36	0.270	0.031	8.606	0.030	0.107

The analysis of this inclusion shows high increase in Al_2O_3% and significant decrease in Na_2O%, SiO_2%, CaO%, and a slight decrease in MgO%. The nearest typical chemical composition to this defect is that for a type of alumina refractories can be considered from mullite class as shown in the following table (note alumina & silica percentages in the following table):

Table 19: Typical chemical composition for a type of alumina refractories from mullite class

OXIDE	SiO_2	Al_2O_3	CaO	MgO	Fe_2O_3
%	50.4	45.4	0.1	0.1	0.9

(Reference: Fay.V.Tooley, "The Hand Book of Glass Manufacture", 3rd edition, Ashlee New York (1984).

The difference between the typical composition of the refractory and the given composition of the defect sample analysis is due to the surrounding glass around the defect.

3.3 Spectrophotometric analysis

The following tables represent the absorption values of glass at 380 nm which is entirely due to Fe_2O_3 in two relations:

1-Relation between absorption & thickness at constant Fe2O3 %

Table 20: absorption & thickness values at constant Fe2O3% in glass

DATE	THICIKNESS (mm)	ABSORPTION VALUES	Fe_2O_3 %
15/04/2002	2.7	0.055	0.102
15/06/2002	2.7	0.055	
19/04/2002	4	0.064	
31/07/2002	5	0.072	
15/08/2002	2.7	0.057	0.112
30/04/2002	8	0.097	
30/08/2002	10	0.112	
15/10/2002	4	0.065	0.106
30/05/2002	5.5	0.073	
30/06/2002	6	0.076	
16/09/2002	5.5	0.076	0.110
28/07/2002	6	0.081	

As shown in table 20 at constant Fe2O3 % by relating absorption values to the thickness, it is observed that as the thickness increases the absorption increases and vice versa.

2- Relation between absorption & Fe2O3 % at constant thickness

Table 21: absorption & Fe2O3 % values at constant thickness

DATE	ABSORPTION VALUES	Fe_2O_3 %	THICIKNESS (mm)
30/09/2002	0.054	0.097	2.7
15/04/2002	0.055	0.102	
15/06/2002	0.055	0.102	
15/08/2002	0.057	0.111	
08/10/2002	0.064	0.100	4
19/04/2002	0.064	0.101	
15/10/2002	0.065	0.106	
31/07/2002	0.072	0.102	5
03/08/2002	0.074	0.116	
30/05/2002	0.073	0.105	5.5
16/09/2002	0.076	0.110	
30/06/2002	0.076	0.106	6
28/07/2002	0.081	0.109	

As shown in table 21 at constant thickness, it is observed that as the Fe_2O_3 % increases the absorption increases and vice versa.